

Programmed Self-Assembly of Heterometallic [3 × 3] Grid [M^{II}Cu^{II}₄Cu^I₄] (M = Fe, Ni, Cu, and Zn)Xin Bao,[†] Wei Liu,[†] Ling-Ling Mao,[†] Shang-Da Jiang,[‡] Jun-Liang Liu,[†] Yan-Cong Chen,[†] and Ming-Liang Tong^{*,†}[†]Key Laboratory of Bioinorganic and Synthetic Chemistry of Ministry of Education, State Key Laboratory of Optoelectronic Materials and Technologies, School of Chemistry and Chemical Engineering, Sun Yat-Sen University, Guangzhou 510275, People's Republic of China[‡]Physikalisches Institut, Universität Stuttgart, Pfaffenwaldring, D-70550 Stuttgart, Germany

Supporting Information

ABSTRACT: A series of heterometallic [3 × 3] grids have been synthesized readily through a one-pot solvothermal reaction. Given metal ions carrying distinct electronic, magnetic, and optical information can be addressed precisely at specific locations in the array.

The self-assembly of grid-type arrays has received considerable attention in recent years because such nanoscale-layered structures are promising candidates for data storage and nanodevices.¹ Particularly, manipulating heterometallic grids with ordered arrangements of specific metal ions is of practical interest. Such well-organized arrays allow information to be written and read out at specific locations. However, reports on heterometallic grids are quite rare.^{2–14} The multicomponent system gives rise to additional difficulties and uncertainties for the self-assembly process. Stepwise synthetic procedures have been explored to construct several heterometallic [2 × 2] grids, generally by introducing metal ions sequentially in the order of increasing coordination lability.^{2–8} One-pot synthesis^{9–11} is an alternative strategy, using a ligand coded with different structural information that can recognize different metal ions.

Previously, we designed and synthesized a series of intriguing homometallic cluster helicates through the self-assembly of a C₂-symmetric tritopic ligand, 2,6-bis[5-(2-pyridinyl)-1H-triazol-3-yl]pyridine (H₂L; Figure 1), with metal (Fe, Mn, or Cd) halogen salts.¹⁵ Coordination chemistry of triazole–pyridine ligands was also well developed by Vos et al.¹⁶ We recently considered that such a bidentate–tridentate–bidentate segmental ligand could also assemble to a [3 × 3] grid if appropriate metal ions are introduced to stabilize the subsequent tetrahedral and square-pyramidal coordination geometries.

Herein we report a programmed one-pot synthesis of a series of heterometallic [3 × 3] grids [M^{II}Cu^{II}₄Cu^I₄L₆]Cl₂·nH₂O [M = Fe (1), Ni (2), Cu (3), and Zn (4) and n = 35–40 for 1–4].¹⁷ Crystals of those complexes were obtained in good yield (c.a. 80%) by the solvothermal reaction of H₂L with CuCl, CuCl₂·2H₂O, and MCl₂·nH₂O in a ratio of 6:4:4:1. In this system, not only can different metal ions be addressed precisely at specific locations in the array but also diverse M^{II} ions can be introduced selectively into the central octahedral coordination site. Namely, Cu^I ions occupy the tetrahedral sites at the corners, Cu^{II} ions take the square-pyramidal sites on the edges, and a third

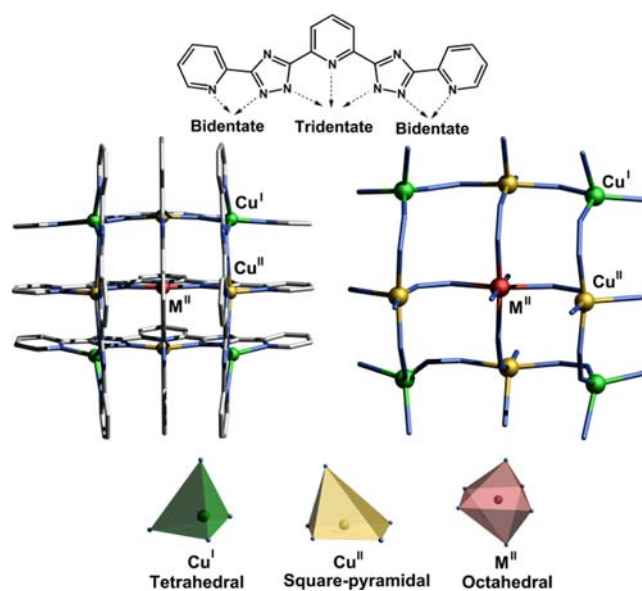


Figure 1. Top: schematic diagram of the tritopic ligand. Middle: crystal structure of the [3 × 3] grid. Color code: Cu^I, green; Cu^{II}, yellow; M^{II}, red; C, gray; N, blue. Bottom: coordination geometries of different metal ions. H atoms are omitted for clarity.

transition-metal ion M^{II} (M = Fe, Ni, Cu, or Zn) sits on the octahedral center.

The composition of the grid cation was confirmed by electrospray ionization mass spectrometry (ESI-MS; Figures S1–S4 in the Supporting Information, SI). The only intense peak with isotopic distributions at *m/z* 1378.0, 1379.0, 1381.5, and 1383.0 for the four complexes corresponds to the nonanuclear heterometallic core [M^{II}Cu^{II}₄Cu^I₄L₆]²⁺ [M = Fe (1), Ni (2), Cu (3), and Zn (4)].

Single-crystal X-ray diffraction measurements were carried out for 1–4. They are isostructural and crystallize in the cubic space group $\bar{I}43m$. The structure of the [3 × 3] cationic grid is shown in Figure 1. As expected, six tritopic ligands arrange in two orthogonal groups above and below the metal planes, resulting in three types of coordination geometries: four tetrahedral

Received: December 20, 2012

Published: May 14, 2013

coordination environments at the corners, four square-pyramidal coordination geometries on the edges, and one octahedral coordination site in the center. Those coordination sites are occupied by four Cu^{I} ions, four Cu^{II} ions, and one M^{II} ion, respectively. The ligands in each group stand in an offset parallel arrangement with separations of ca. 3.3 Å, indicating the presence of strong π - π interactions (Figure S5 in the SI). The two diagonal Cu^{I} ions have the same chirality and are heterochiral to the other two Cu^{I} ions, resulting in a mesomeric cation. A total of 18 grid molecules occupy 12 edges and 6 faces of the cubic unit cell, forming a nanocage with the diameter of ca. 15 Å (Figure S6 in the SI), which is occupied by disordered Cl^- anions and water molecules.

In this series of $[3 \times 3]$ grids, such a high toposelectivity toward specific metal ions is mainly attributed to their different coordination preferences: Cu^{I} predominantly exhibits a tetrahedral geometry, whereas Cu^{II} favors a square-planar geometry or a five- or six-coordination format;¹⁸ Fe^{II} , Ni^{II} , and Zn^{II} ions give abundant examples of octahedral coordination geometry. It has been well acknowledged that coordination algorithms between ligands and metal ions play an important role in the self-assembly process.¹⁹ The controlled synthesis of different metalloarchitectures reported by Lehn et al. is a nice example showing that reasonable utilization of coordination algorithms may allow the directed generation of specific and predictable architectures. In their case, the long and flexible ligand containing bidentate and tridentate subunits requires either a set of tetrahedral + octahedral coordinated metal ions or tetrahedral + trigonal-bipyramidal coordinated metal ions.^{20–22} Here, in comparison, the combination of six relatively short and rigid ligands requires three kinds of coordinated metal ions: tetrahedral + square-pyramidal + octahedral. It should be noted that Cu^{I} ions always appear in the final product regardless of whether they are involved as the starting reagent, which may be attributed to an in situ reduction of Cu^{II} ions. In addition to the coordination geometry factor, such a composition is also stabilized by a lower charge preference, namely, a 2+ charge for the $[\text{M}^{\text{II}}\text{Cu}_4^{\text{II}}\text{Cu}_4^{\text{I}}\text{L}_6]$ cation versus a 6+ charge for the $[\text{M}^{\text{II}}\text{Cu}_8^{\text{II}}\text{L}_6]$ cation. However, if neither Cu^{I} nor Cu^{II} ions are introduced, the grid-type structure could not be obtained, at least in the same or similar conditions, because of the mismatch for the tetrahedral and square-pyramidal coordination sites. Concerning the central position, it can accommodate a variety of metal ions, including Fe^{II} , Ni^{II} , Cu^{II} , and Zn^{II} . The coordination geometry of this site is regular and highly constrained because of the specific arrangement of the ligands and thus is disliked by the Cu^{II} ion with a Jahn–Teller distortion tendency. Consequently, the third M^{II} ion will take the site in priority to Cu^{II} instead of forming a solid solution. It is interesting to note that the Fe^{II} ion in complex 1 stays in the low-spin state in the entire operating temperature range (average Fe–N bond length is 1.95 Å), although it is usually found to exhibit a temperature-dependent spin transition when wrapped by similar 2,6-dipyrazolylpyridine fragments.^{23,24} Stabilization of the low-spin state may also be ascribed to structural restriction. For the same reason, the insertion of ions with larger radii such as lanthanide was unsuccessful.

The existence of Cu^{I} and Cu^{II} as well as the third metal ion was confirmed by X-ray photoelectron spectrometry (XPS) analysis (Figures 2 and S7 and S8 in the SI). The peaks at 954.7 and 934.8 eV were assigned to the $2p_{1/2}$ and $2p_{3/2}$ doublet of the Cu^{II} ion. The satellite peak around 943 eV corresponds to the typical shakeup line that chemically denotes the Cu^{II} oxidation state. The $2p_{1/2}$ and $2p_{3/2}$ doublet of Cu^{I} was observed at 951.7 and

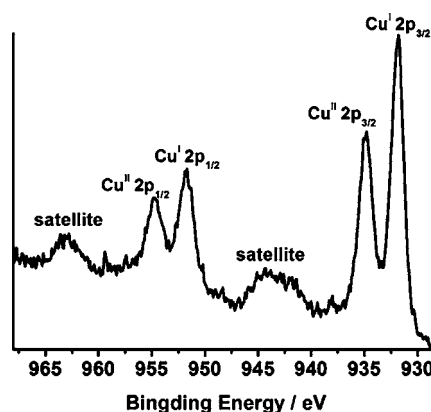


Figure 2. XPS spectrum of the Cu 2p level revealing the presence of Cu^{I} and Cu^{II} .

931.8 eV. The $2p_{3/2}$ peaks of Fe, Ni, and Zn in complexes 1, 2, and 4 appear at 710.3, 855.5, and 1021.3 eV, respectively. The $2p_{3/2}$ peak of the Cl^- counteranion was observed at 196.2 eV.

Inductively coupled plasma atomic emission spectroscopy was carried out in order to confirm the ratio of different metal ions. Cu/Fe, Cu/Ni, and Cu/Zn molar ratios are 7.94, 8.04, and 7.88, respectively, which are consistent with the 8:1 ratio deduced from other measurements.

Electron paramagnetic resonance (EPR) spectra were performed on frozen solutions of 1–4 at 5 K (Figure 3). 1, 3,

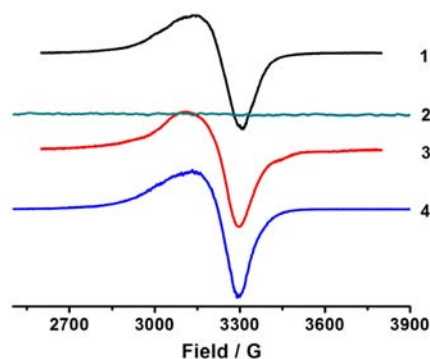


Figure 3. EPR spectra of 1–4 measured at 5 K on freshly prepared solution samples. Experimental settings: microwave frequency, 9.47 GHz; microwave power, 0.01 mW; field modulation, 0.2 mT.

and 4 display a typical EPR signal with $g = 2.093$, 2.098, and 2.100, respectively, corresponding to the paramagnetic Cu^{II} ions in the grids. No hyperfine splitting was resolved. 2 is EPR-silent, denoting an integer spin ground state due to antiferromagnetic coupling between the central Ni^{II} and surrounding Cu^{II} ions (see the following magnetic studies). Variable-temperature magnetic susceptibility behaviors of those complexes are dependent on the central metal ion (Figure 4). 1 and 4 show almost constant $\chi_{\text{M}}T$ values of ca. 1.6 emu K mol^{-1} between 300 and 2 K, corresponding to four isolated Cu^{II} ions. Magnetic coupling is blocked by the diamagnetic Cu^{I} ions at the corners and Fe^{II} (in the low-spin state) or Zn^{II} ions in the center. In the cases of 2 and 3, their $\chi_{\text{M}}T$ values decrease upon cooling because of antiferromagnetic coupling between the central paramagnetic metal ion and the four Cu^{II} ions. Fitting the experimental curves of 2 (above 20 K) and 3 by the Hamiltonian model²⁵ (see the SI for details) gives $J = -4.46 \text{ cm}^{-1}$, $zJ = -0.2 \text{ cm}^{-1}$ and $g = 2.17$, for 2 and $J = -3.68 \text{ cm}^{-1}$ and $zJ = -0.55 \text{ cm}^{-1}$ with a fixed g value of

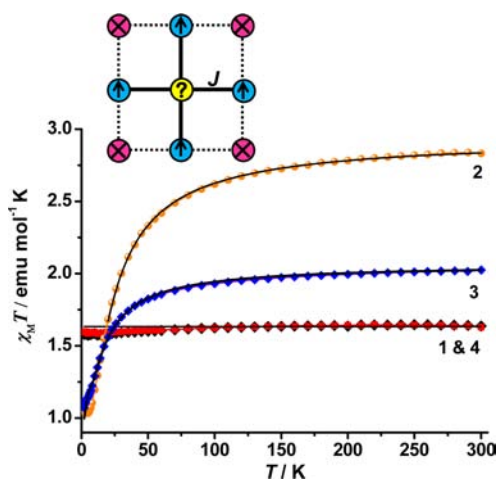


Figure 4. Temperature dependence of $\chi_M T$ measured in an applied field of 5000 Oe on polycrystalline samples of 1–4. The solid lines represent the best-fitting curves. Inset: magnetic exchange coupling pathways in those complexes.

2.098 for 3, where J corresponds to an exchange coupling constant between the central metal ion and Cu^{II} ions on the edges and zJ represents intercluster magnetic coupling.

The $-\text{H}$ plots of 1–4 were well reproduced using energy levels calculated by the above mentioned fitting parameters (Figure S11–S13 in the SI).

The UV–vis spectra of 1–4 in a MeOH solution show similar shapes (Figure S9 in the SI). The intense absorption bands in the UV region at 240 and 280 nm are ligand-centered transitions. The weak band at 400 nm with a shoulder at 330 nm could be assigned to Cu^{I} -to-ligand charge-transfer (MLCT) transition. For complex 1, there is an additional band centered at 490 nm, which is reasonably attributed to MLCT from Fe^{II} to ligand. The absorption spectra explain the color of those complexes: reddish for 1 and yellowish green for 2–4 (Figure S9 in the SI).

In summary, as a forward step in the construction of a heterometallic $[2 \times 2]$ grid, we presented a successful one-pot self-assembly of a multicomponent $[3 \times 3]$ grid. Different metal ions can be addressed precisely at specific positions based on different binding preferences. Particularly, the central metal ion can be altered systematically, thus allowing an easy modification of the magnetic, electronic, and optical properties of the grid. Such a well-organized heterometallic grid with controllable properties is of practical interest for the development of molecular information storage and processing devices.

■ ASSOCIATED CONTENT

Supporting Information

Materials and general procedures, synthesis, X-ray crystallography, fitting details for experimental magnetic susceptibility curves, ESI-MS, XPS, and EPR spectra, thermogravimetric (TG) curves, spin-energy-level spectra, supplementary structural figures, and selected bond lengths. This material is available free of charge via the Internet at <http://pubs.acs.org>.

■ AUTHOR INFORMATION

Corresponding Author

*E-mail: tongml@mail.sysu.edu.cn.

Notes

The authors declare no competing financial interest.

■ ACKNOWLEDGMENTS

This work was supported by the 973 Project (Grant 2012CB821704), the NSFC (Grants 91122032, 21121061, and J1103305), and the Yat-sen Innovative Talents Cultivation Program for Excellent Tutors. We thank Dominik Dengler and Prof. Joris van Slageren, Institut für Physikalische Chemie, Pfaffenwaldring 55, 70569 Stuttgart, Germany, for the help with the low temperature EPR measurements.

■ REFERENCES

- (1) Ruben, M.; Rojo, J.; Romero-Salguero, F. J.; Uppadine, L. H.; Lehn, J.-M. *Angew. Chem., Int. Ed.* **2004**, *43*, 3644.
- (2) Bassani, D. M.; Lehn, J.-M.; Fromm, K.; Fenske, D. *Angew. Chem., Int. Ed.* **1998**, *37*, 2364.
- (3) Xu, Z.; Thompson, L. K.; Matthews, C. J.; Miller, D. O.; Goeta, A. E.; Howard, J. A. K. *Inorg. Chem.* **2001**, *40*, 2446.
- (4) Bassani, D. M.; Lehn, J.-M.; Serroni, S.; Puntoriero, F.; Campagna, S. *Chem.—Eur. J.* **2003**, *9*, 5936.
- (5) Uppadine, L. H.; Lehn, J.-M. *Angew. Chem., Int. Ed.* **2004**, *43*, 240.
- (6) Uppadine, L. H.; Gisselbrecht, J.-P.; Kyritsakas, N.; Näntinen, K.; Rissanen, K.; Lehn, J.-M. *Chem.—Eur. J.* **2005**, *11*, 2549.
- (7) Parsons, S. R.; Thompson, L. K.; Dey, S. K.; Wilson, C.; Howard, J. A. K. *Inorg. Chem.* **2006**, *45*, 8832.
- (8) Stefankiewicz, A. R.; Harrowfield, J.; Madalan, A.; Rissanen, K.; Sobolevc, A. N.; Lehn, J.-M. *Dalton Trans.* **2011**, *40*, 12320.
- (9) Petitjean, A.; Kyritsakas, N.; Lehn, J.-M. *Chem. Commun.* **2004**, 1168.
- (10) Moroz, Y. S.; Szyrwiel, L.; Demeshko, S.; Kozłowski, H.; Meyer, F.; Fritsky, I. O. *Inorg. Chem.* **2010**, *49*, 4750.
- (11) Newton, G. N.; Onuki, T.; Shiga, T.; Noguchi, M.; Matsumoto, T.; Mathieson, J. S.; Nihei, M.; Nakano, M.; Cronin, L.; Oshio, H. *Angew. Chem., Int. Ed.* **2011**, *50*, 4844.
- (12) Zhao, Y.; Guo, D.; Liu, Y.; He, C.; Duan, C. *Chem. Commun.* **2008**, 5725.
- (13) Dawe, L. N.; Shuvaev, K. V.; Thompson, L. K. *Inorg. Chem.* **2009**, *48*, 3323.
- (14) Shiga, T.; Matsumoto, T.; Noguchi, M.; Onuki, T.; Hoshino, N.; Newton, G. N.; Nakano, N.; Oshio, H. *Chem.—Asian J.* **2009**, *4*, 1660.
- (15) Bao, X.; Liu, W.; Liu, J.-L.; Gómez-Coca, S.; Ruiz, E.; Tong, M. L. *Inorg. Chem.* **2013**, *52*, 1099.
- (16) For example, see: Browne, W. R.; Heseck, D.; Gallagher, J. F.; O'Connor, C. M.; Killeen, J. S.; Aoki, F.; Ishida, H.; Inoue, Y.; Villani, C.; Vos, J. G. *Dalton Trans.* **2003**, 2597.
- (17) n is an uncertain value because some solvent water molecules may escape from the large void once the crystals are taken away from the mother liquid. Thus, it is a value dependent on the storage temperature, humidity, and time after being removed from the mother solvent. The number report in the text was based on TG analyses.
- (18) Collin, J.-P.; Dietrich-Buchecker, C.; Gaviña, P.; Jimenez-Molero, M. C.; Sauvage, J.-P. *Acc. Chem. Res.* **2001**, *34*, 477.
- (19) Lehn, J. M. *Supramolecular Chemistry: Concepts and Perspectives*; VCH: Weinheim, Germany, 1995.
- (20) Funeriu, D. P.; Lehn, J.-M.; Fromm, K. M.; Fenske, D. *Chem.—Eur. J.* **2000**, *6*, 2103.
- (21) Lehn, J.-M. *Chem.—Eur. J.* **2000**, *6*, 2097.
- (22) Lehn, J.-M. *Science* **2002**, *295*, 2400.
- (23) Halcrow, M. A. *Coord. Chem. Rev.* **2005**, *249*, 2880.
- (24) Halcrow, M. A. *Coord. Chem. Rev.* **2009**, *253*, 2493.
- (25) Freedman, D. E.; Jenkins, D. M.; Iavarone, A. T.; Long, J. R. *J. Am. Chem. Soc.* **2008**, *130*, 2884.